

The quantum superluminality in the tunnel-ionization process of H-like atoms

Ossama Kullie¹ and Igor A. Ivanov²

¹ *Institute for Physics, Department of Mathematics and Natural Science, University of Kassel, Germany and*

² *Department of Fundamental and Theoretical Physics, Australian National University, Australia.**

The quantum tunneling time remains the subject of heated debate, and one of its most curious features is faster-than-light or superluminal tunneling. Our tunnel-ionization model of the time-delay, presented in previous work, shows good agreement with the attoclock measurement in the adiabatic and nonadiabatic field calibrations, which also enables the determination of the barrier time-delay. In the present work, we show that the tunnel-ionization for H-like atoms with large nuclear charge can be superluminal (quantum superluminality), which in principle can be investigated experimentally using the attoclock scheme. We discuss the quantum superluminality in detail for the different regimes of the tunnel-ionization. Our result shows that quantum tunneling faster-than-light is indeed possible, albeit only under somewhat extreme conditions.

Keywords: Ultrafast science, attosecond physics, tunneling and tunnel-ionization time-delay, nonadiabatic effects, weak measurement, interaction time, superluminal tunneling, time and time-operator in quantum mechanics.

I. INTRODUCTION

The interaction of an atom with a laser pulse in strong-field and attosecond physics can be represented in a simplified picture, as shown in Fig. 1, which illustrates the main features of the interaction in the tunnel-ionization regime. In previous work we developed in [1, 2] a tunneling time-delay model, which explains the measurement result of the attoclock, in the adiabatic [3] and nonadiabatic [4] field calibrations. In the model, upon interacting with the electric field of the laser (hereafter field strength) F , a direct ionization happens when the field strength reaches a threshold called atomic field strength $F_a = I_p^2/(4Z_{eff})$ [5, 6], where I_p is the ionization potential of the system (atom or molecule) and Z_{eff} is the effective nuclear charge in the single-active electron approximation (SAEA), and atomic units (au) with $\hbar = m = e = 1$ are used throughout the present work. However, for $F < F_a$ the ionization can happen by tunneling through a potential barrier $V_{eff}(x) = V(x) - xF = -\frac{Z_{eff}}{x} - xF$, compare Fig. 1. In the model the tunneling process is described with the help of the quantity $\delta_z = \sqrt{I_p^2 - 4Z_{eff}F}$, where F stands (throughout this work) for *the peak electric field strength at maximum*. In Fig. 1 (for details see [1]), the inner (entrance $x_{e,-}$) and outer (exit $x_{e,+}$) points are given by $x_{e,\pm} = (I_p \pm \delta_z)/(2F)$, the barrier width is $d_B = x_{e,+} - x_{e,-} = \delta_z/F$, and its (maximum) height (at $x_m(F) = \sqrt{Z_{eff}/F}$) is δ_z . At $F = F_a$, we have $\delta_z = 0$ ($d_B = 0$), the barrier disappears and the direct or the barrier-suppression ionization starts, green (dashed-dotted) curve in Fig. 1.

a. Adiabatic tunneling: In the adiabatic field calibration of the attoclock of Landsman et. al. [3], we showed in [1] that the tunneling time (T-time)-delay is described by

the forms,

$$\tau_{T,d} = \frac{1}{2(I_p - \delta_z)}, \quad \tau_{T,i} = \frac{1}{2(I_p + \delta_z)} \quad (1)$$

It was shown that $\tau_{T,d}$ has a good agreement with the experimental result of Landsman et. al. [3]. $\tau_{T,d}$ is the time-delay of the adiabatic tunnel-ionization whereas $\tau_{T,i}$ is the time needed to reach the entrance point $x_{e,-}$. At the limit of

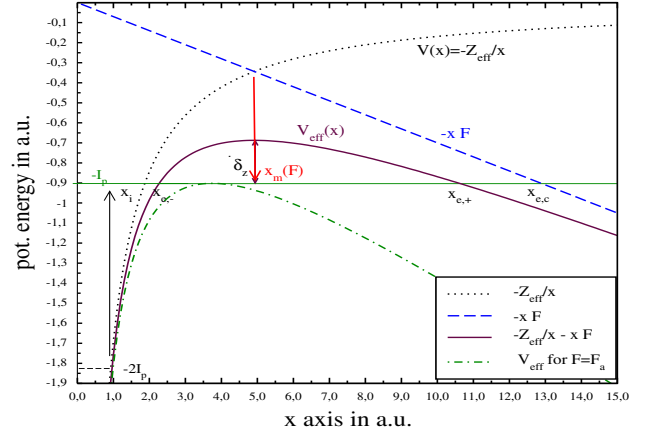


FIG. 1. (Color online) A sketch of the atomic and the effective potential curves, showing the height and width of the barrier formed by the interaction with the laser field. The plot is for He-atom in the SAEA model with $Z_{eff} = 1.6875$ and $I_p \approx 0.9$ au.

atomic field strength, we have $\lim_{F \rightarrow F_a} (\delta_z \rightarrow 0) \tau_{T,d} = \tau_{T,i} = \frac{1}{2I_p} = \tau_a$ (see below). For $F > F_a$, the barrier-suppression ionization sets up [7, 8]. On the opposite side, we have $\lim_{F \rightarrow 0} (\delta_z \rightarrow I_p) \tau_{T,d} \rightarrow \infty$. So nothing happens and the electron remains in its ground state undisturbed, which shows that our model is consistent. For details, see [1, 9–11].

b. Nonadiabatic tunneling: In the nonadiabatic field calibration of Hofmann et. al. [4] for He-atom, we showed

* Email: kullie@uni-kassel.de

in [2] that the time-delay is given by

$$\tau_{dion}(F) = \frac{1}{2 \cdot 4Z_{eff}} \frac{I_p}{F} = \frac{1}{2I_p} \frac{F_a}{F} \quad (2)$$

with good agreement with the experimental result. It is easily seen that in the limit $F \rightarrow F_a$, $\tau_{dion} = \tau_a$, whereas in the opposite case $F \rightarrow 0$, $\tau_{dion} = \infty$. τ_a is always (adiabatically and nonadiabatically) a lower quantum limit of the tunnel-ionization time-delay and quantum mechanically does not vanish.

c. Barrier time-delay: Eq. 1 can be decomposed into a twofold time-delay with respect to ionization at F_a , representing the T-time-delay in an unfolded form,

$$\tau_{T,d} = \tau_a \frac{F_a}{F} + \tau_a \frac{F_a}{F} \frac{\delta_z}{I_p} = \tau_{dion}(F) + \tau_{dB} \equiv \tau_{Ad} \quad (3)$$

From now on, we will refer to it as $\tau_{Ad} \equiv \tau_{T,d}$. The first term of Eq. 3, which is identical to Eq. 2, is a time-delay enhancement solely because F is smaller than F_a , whereas the second term τ_{dB} is a time-delay enhancement due to the barrier itself, it is the actual T-time-delay, usually referred to as the time spent within the barrier [12], which agrees well with the numerical models of Winful [13] and Lunardi [14] and the experimental result based on two field calibrations mentioned above, as shown in [12]. The conclusion is that Eq. 3 represents a unified T-time picture (UTTP) [12, 13] with $\tau_{dB} = \tau_{dwell}$ and is determined by

$$\tau_{Ad} - \tau_{dion} = \tau_{dB} = \frac{1}{2} \frac{1}{4Z_{eff}} \frac{\delta_z}{F} = \frac{1}{2} \frac{d_B}{4Z_{eff}} \quad (4)$$

Obviously, Eq. 4 gives the time spent within the barrier $\tau_{barrier}$ [12–14] or the dwell time τ_{dwell} [13]. It shows a linear dependence of the τ_{dB} on the barrier width d_B , which tends to zero in the limit of $F = F_a$ ($\delta_z = 0$) because the barrier disappears [15]. A similar linear dependence on the barrier width is shown by Balcou [16] for the phase-time in optical tunneling. Unfortunately, τ_{dB} cannot be measured by the experiment directly since the first term τ_{dion} is always present. However, as seen in Eq. 4, it can be determined taking into account both field calibrations, as shown in [12]. See further below Fig. 3.

d. thick-barrier and Weak measurement In the limit of a thick (or opaque) barrier, the barrier width approaches the so-called classical barrier width d_C , $\lim_{F \ll F_a} d_B \approx I_p/F = d_C(x_{e,c})$, compare Fig. 1. In this limit the barrier height $\lim_{F \ll F_a} \delta_z \rightarrow I_p$, and the barrier time

$$\begin{aligned} \lim_{F \ll F_a} \tau_{dB} &= \tau_a \frac{F_a}{F} \frac{(\delta_z \approx I_p)}{I_p} \approx \tau_a \frac{F_a}{F} = \tau_{dion} \quad (5) \\ &= \frac{1}{2} \frac{1}{4Z_{eff}} \frac{I_p}{F} = \frac{1}{2} \frac{d_C}{4Z_{eff}} \end{aligned}$$

The result shows that the barrier time-delay τ_{dB} for a thick-barrier (or opaque barrier) is approximately equal to tunnel-ionization time-delay τ_{dion} of Eq. 2. In addition, the

back reaction of the measurement of the system can be found from $\tau_{T,i}$ as the following $\lim_{F \ll F_a} \tau_{T,i} = \frac{1}{2} \frac{(I_p - \delta_z)}{4Z_{eff}F} = \frac{1}{2} \frac{\varepsilon_F}{4Z_{eff}F} = \tau_{backr}$, where $\varepsilon_F = \delta_z - I_p$ is small under the condition a weak measurement ($F \ll F_a$). However, the condition of WM is not necessary and we can assume that τ_{backr} always represents the back reaction of the system, although it can be generally interpreted as the time needed to reach the barrier entrance in the strong-field interaction as already mentioned [12].

II. THE QUANTUM SUPERLUMINALITY

Superluminal tunneling or (quantum) superluminality, which means that the T-time of a barrier can be a shorter than that of light passing through a vacuum over the same distance of the barrier width (superluminal speed), is one of the most exciting and controversial phenomena in quantum physics. In photonic tunneling many authors reported that they measured superluminal T-time experimentally. They also argued that it does not violate the principle of causality or special relativity [17–21]. In his explanation of tunneling of light pulses through a barrier (Nature of ‘‘Superluminal’’ Barrier Tunneling) [13, 22, 23], Winful argued that the measured T-time is not a propagation time and, if interpreted correctly, no superluminal transport would be observed. He claims that what is really observed then is a phase shift in an amplitude modulation. Büttiker et. al. [24] believe that it is just an artifact of our definition of speed as marked by the arrival of the peak in the pulse, whereas Steinberg et. al. [25] suggest that the group delay (or ‘‘phase time’’) gives a better description of the physically observable delay.

In quantum tunneling of a stream of particles that scatters at a potential barrier, Winful [13] (see sec. 1.0c) showed that the group delay is equal to the dwell time plus a self-interference time-delay. The Hartman effect in quantum tunneling, which says that the phase time of tunneled particles is independent of barrier width for sufficiently wide (thick) barrier, is explained on the basis of saturation of the integrated probability density (or number of particles) under the barrier. More recently Dumont et. al. [19] investigate the MacColl-Hartman (or Hartman) effect [15, 26]. They showed that the phase time is the appropriate way of measuring the barrier interaction time and it can lead to faster-than-light time. However, they claim that only the statistics of the arrival time of the particles distribution can be used to make statements. They conclude that their analysis leads to the impossibility of superluminal signaling using the MacColl-Hartman effect [19].

Nanni [27], on the other hand, recently reported the possibility of superluminal transport of electromagnetic energy in photonic tunneling. And what’s even more exciting: Lunardi et. al. [14] provide, a plausible explanation for a possible superluminal tunneling process in the attoclock framework using numerical simulation.

Based on our model, below we study the superluminality in the attoclock framework, where we refer to it as quantum

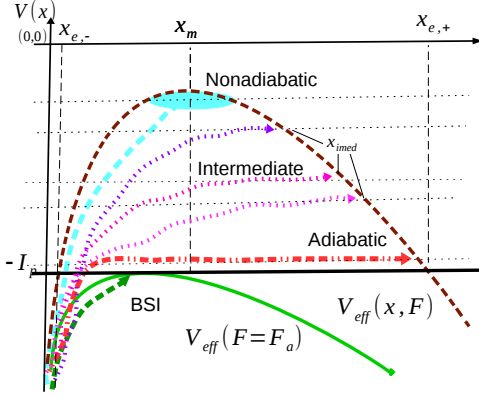


FIG. 2. (Color online) Outline of tunnel-ionization in three cases: adiabatic (dashed-dotted, red), intermediate (dotted, magenta, purple) and nonadiabatic (dashed, light blue). As well as the barrier-suppression ionization at F_a (green).

superluminality (QS), with the conclusion that superluminality is quite possible, albeit under somewhat “extreme” conditions. The advantage of our model in explaining the attoclock measurement lies in the simplicity of determining the tunnel-ionization time-delay in the adiabatic and nonadiabatic field calibrations and allows the extraction of the barrier time-delay. It gives a clear picture of tunneling in general and emphasizes the UTTP in particular, in line with the approaches of Winful [13] and Lunradi [14, 28] explained above, see sec. I 0 c.

The measurement of the attoclock experiment offers two field calibrations based on adiabatic or nonadiabatic tunneling theory. However, the tunneling process can also be described by an intermediate regime in which adiabatic and nonadiabatic tunnel-ionization coexists [29]. This is shown in Fig. 2 by dotted (magenta or purple colored) curves. To investigate the QS, we first discuss the adiabatic and nonadiabatic cases for which experimental results are available and later will deal with the intermediate regime, which is formulated into a generalized model using a switching parameter. The final result will then be presented based on this model.

A. QS in adiabatic tunnel-ionization

a. Barrier time-delay Adiabatic tunneling happens along the so-called horizontal channel, as shown in Fig. 2 (dashed-dotted red colored), where the exit point is at $x_{e,+}$ (compare Fig. 1) and the barrier width is $d_B = \frac{\delta_z}{F}$. The barrier time-delay itself $\tau_{dB} = \frac{d_B}{8Z_{eff}}$ shows a linear dependence on the barrier width [12, 15], in contrast to the Hartman effect, i.e. the lack of dependence of T-time-delay on barrier length for thick (opaque) barrier as discussed in [22]. Therefore, it is to be expected that, within the framework of the attoclock, even in the limit of a thick-barrier, no superluminal tunneling takes place. This is indeed true in experiments when considering the light atoms under investigation, such as the He atom as shown in [1, 3, 30].

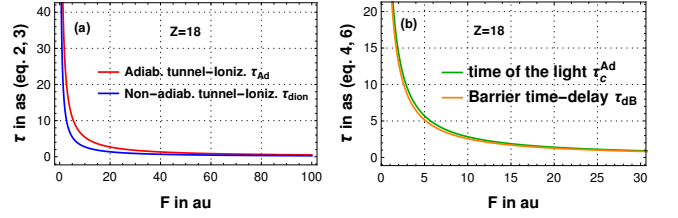


FIG. 3. (Color online) (a): Tunnel-ionization time-delay in the adiabatic and nonadiabatic field calibration τ_{Ad}, τ_{dion} vs. field strength F (in au) for $Z = 18$. (b): Time-delay of the barrier τ_{dB} (green) and the time of light τ_c^{Ad} (orange) vs. field strength F (in au) for $Z = 18$, see Eq. 6. Hereafter “as” is the abbreviation for attosecond.

It can be seen if one compares the time-delay τ_{dB} with the time required for the light, to overcome the barrier width d_B with the speed c in vacuum $\tau_c^{Ad} = \frac{d_B}{c}$, where one can easily verify that $\tau_{dB}/\tau_c^{Ad} = c/(8Z_{eff}) > 1$ for $Z_{eff} = 1.6875$ [31] (or $Z_{eff} = \sqrt{2}I_p = 1.344$).

However, a closer look at τ_{dB} and τ_c^{Ad} indicates that the tunneled electron traverses the barrier region with an average speed of $v_{av} = 8Z_{eff}$. The comparison of τ_{dB} (Eqs. 4-5) and the corresponding travel time of the light τ_c^{Ad} leads to the following condition for the occurrence of superluminal tunnel-ionization,

$$Q_{dB} = \frac{\tau_{dB}}{\tau_c^{Ad}} = \frac{c}{8Z_{eff}} < 1 \Rightarrow Z_{eff} > c/8 \approx 17.13 \quad (6)$$

where $c = 173.0359992$ (CODATA22). This indicates that the barrier tunneling time-delay τ_{dB} can be superluminal, or that the QS occurs when the strength of the nuclear potential large and $Z_{eff} \geq 18$ holds. Fig. 3 (a) shows τ_{dion} (Eq. 2) and τ_{Ad} (Eq. 3) as a function of the field strength for one-electron H-like ionic Argon Ar^{+17} where $Z_{eff} = Z = 18$, while their difference, i.e. the barrier time-delay τ_{dB} (Eq. 4), is shown in Fig. 3 (b) together with the light travel time τ_c^{Ad} through the barrier width (see text above Eq. 6), from which it is clearly evident that the barrier time-delay τ_{dB} becomes smaller than τ_c^{Ad} for $Z \geq 18$. Indeed, τ_{dion} and τ_{Ad} become very small for large field strength F , but Eqs. 4-5 and the corresponding condition of Eq. 6 are always satisfied for $F \leq F_a$, see further below. In A2 we present result from the numerical integration of the time-dependent Schrödinger equation (NITDSE). For $Z = 18$ and $F = 50/\sqrt{2} a.u.$, $\omega = 3 a.u.$, we obtained a time-delay of $\tau \approx 4 a.s.$ Unfortunately, this differs from the result obtained from our model $\tau_{dB} \approx \tau_{dion} \approx 0.7 a.s.$ we are not able to explain this discrepancy at the moment.

For the rest of the present work, we discuss H-like atoms $A^{+(Z-1)}$ in the ground state ($Z_{eff} = Z$), where Z is the nuclear charge of the atom A, e.g. He^+ , Li^{+2} , ..., with the nonrelativistic ionization potential $I_p = Z^2/2$. In this case, the barrier height $\delta_z = \sqrt{I_p^2 - 4ZF} = Z^2/2\sqrt{1 - F/F_a} = Z^2/2\sqrt{1 - 16F/Z^3}$ increases with Z^2 (relativistic effect are not crucial and can be taken into account, see below). For large Z the second term under the square root is small for $F \ll F_a = Z^3/16$ and the barrier width $d_B = \delta_z/F$ increase

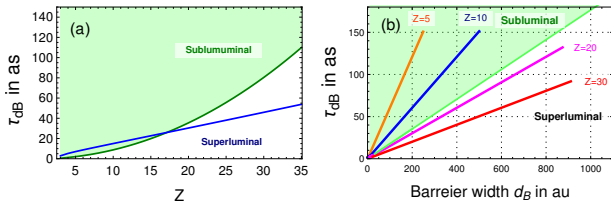


FIG. 4. (Color online) (a): tunnel-ionization τ_{dB} (Eq. 4) vs. Z for $F = 1 au$. The green/white area is subluminal/superluminal. (b): τ_{dB} vs. barrier width $d_B(F)$ for different Z -values. The boundary between subluminal area (green) and superluminal area (white) is along $Z = c/8$, see Eq. 6.

with Z^2 for fixed F and both the height and width of the barrier become too large for large Z . In general, for large Z in the Attoclock framework, where $F \ll F_a = Z^3/16$, the limit of a thick (or opaque) barrier applies.

In Fig. 4 (a), we let Z increases as a parameter and plot $\tau_{dB}(Z)$ (blue) together with $\tau_c^{Ad}(Z)$ (green), where we used the value of $F = 1 au$. It is clearly seen that the barrier time-delay is subluminal for $Z < 18$ (green area). Whereas the blue colored line or τ_{dB} becomes superluminal for $Z \geq 18$ (white area). The part of the blue curve in the green area applies for $Z \leq 17$ and the intersection point marks the value $Z = c/8$. It is worth noting that a change in F -value does not alter the overall appearance in Fig. 4 (a) provided we choose $F < F_a$ for the smallest Z in each case, where we started in Fig. 4 (a) with $Z = 3$ ($F_a \approx 1.7 au$).

In Fig. 4 (b), we plot τ_{dB} vs. the barrier width for various Z -values. As can be seen in Fig. 4 (b), τ_{dB} increases linearly with the barrier width d_B . The green colored area represents the subluminal tunnel-ionization, and the boundary τ_c^{Ad} with $Z = c/8$ (see Eq. 6) marking the transition to superluminal tunnel-ionization. For $F \rightarrow F_a$, we have $\tau_{dB} = \tau_c^{Ad} = 0$ because the barrier disappears, as is known from the Hartman effect. However, the linear dependence of τ_{dB} on the barrier width contrasts the Hartman-effect for thick-barrier (with $F \ll F_a \approx Z^3/16$), which makes the above mentioned argument of Winful [22] not applicable (first paragraph of sec. II). On the other hand, for a fixed barrier width d_B , τ_{dB} decreases with increasing barrier height δ_z (increasing Z), as can be seen from Eq. 4 (a vertical cut line for a chosen d_B -value in Fig. 4 (b)). This agrees with the observation of Spierings et. al. [32]. Using the Larmor clock (LC) measurement for atoms tunneling through an optical barrier, they found that atoms generally spend less time tunneling through a higher barrier. It appears that we are dealing here with a universal behavior that is consistent with the time-energy uncertainty principle.

b. Adiabatic time-delay Our comparison so far concern only the barrier time-delay, while the measurement in the adiabatic field calibration provides the time-delay τ_{Ad} given in Eq. 3, which is the relevant (measurement) physical quantity to be compared with τ_c^{Ad} . It includes the time-delay τ_{dion} and the barrier time-delay τ_{dB} given in Eq. 3. This shifts the boundary of QS of the adiabatic time-delay of tunnel-ionization that can be experimentally measured.

For thick-barrier $\delta_z \approx I_p \Rightarrow \tau_{Ad} \approx \frac{I_p}{4ZF}$, and after some manipulation, as previously done, we obtain that QS occurs when

$$Q_{ad} = \tau_{Ad}/\tau_c^{Ad} < 1 \Rightarrow Z > c/4 \approx 34.26 \quad (7)$$

This shows that quantum superluminality is possible in adiabatic tunneling, albeit under somehow extreme conditions $Z \geq 35$ where the probability of the tunneling in question is most likely very low, as is known from quantum tunneling [14, 19, 33].

We conclude that QS is a fundamental property of adiabatic tunnel-ionization, since our model is consistent and exhibits a universal behavior in accordance with the unified tunneling picture proposed by Winful [13, 14, 28], and is well supported by the agreement of the barrier time-delay with the LC time-delay measurement [32], compare sec. I 0 d the limit of thick-barrier.

B. QS in nonadiabatic tunnel-ionization

Nonadiabatic tunnel-ionization happens along the vertical channel, as shown in Fig. 2 (light blue curve), where the exit point is $x_m = \sqrt{Z/F}$ at the top of the barrier. This changes the situation as the width traversed becomes significantly shorter $d_m \approx x_m$, where the initial point $x_{e,-}$ is small and can be neglected. In this case the time-delay is given by $\tau_{dion} = \frac{1}{8Z} \frac{I_p}{F} \approx \frac{Z}{16F} = \frac{1}{16} x_m^2$ (the relativistic effect changes it slightly). We will first compare our τ_{dion} with $\tau_c^{Ad} = d_B/c$ and later do the same for $\tau_c^{Nad} = \frac{d_m}{c} \approx \frac{x_m}{c}$, where the traversed width of the non-adiabatic tunnel-ionization (the vertical channel) at the exit point $d_m = x_m$ is assumed.

a. With τ_c^{Ad} : For thick-barrier $\delta_z \approx I_p$, $d_B \approx d_C = I_p/F$, $\tau_c^{Ad} = d_C/c$ and after some manipulation, we get a similar result to Eq. 6 ($Z < 17.13$) showing that QS is possible in the nonadiabatic tunnel-ionization. However, τ_{dion} in the nonadiabatic tunnel-ionization is an interaction time (multiphoton absorption) and not a transverse time along the barrier width d_B (x -axis direction). The comparison of τ_{dion} (vertical channel) with the travel time of the light through the barrier width d_B (horizontal channel) is fictitious in this case; in other words, our comparison with τ_c^{Ad} is inappropriate.

b. With τ_c^{Nad} : Rather, one has to compare τ_{dion} with $\tau_c^{Nad} = d_m/c \approx x_m/c$, which is the time it takes for the light to traverse the distance $d_m \approx x_m$ horizontally. In this case with $I_p \approx Z^2/2$, QS is possible if

$$\begin{aligned} Q_{Nad} &= \tau_{dion}/\tau_c^{Nad} = \frac{I_p}{8ZF} \frac{c}{x_m} \\ &= \frac{I_p c}{8ZF} \sqrt{F/Z} \approx \frac{c}{16} \sqrt{Z/F} = \frac{c}{16} x_m < 1 \end{aligned} \quad (8)$$

This leads to the condition $F > (c/16)^2 \cdot Z \approx 73.36 Z$, and together with the condition $F \leq F_a \approx \frac{Z^3}{16}$ (the tunneling

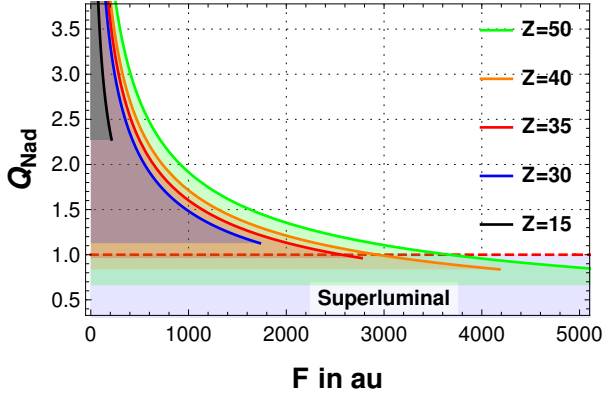


FIG. 5. (Color online) Q_{Nad} (see Eq. 8) vs. field strength F (in au) for various Z values. In the colored area below the red dashed line, tunnel-ionization is superluminal, which is the case when $Z \geq 35$.

regime) we get,

$$\begin{aligned} F_c &= (c/16)^2 Z < F \leq Z^3/16 & (9) \\ \Rightarrow (c/16)^2 Z < Z^3/16 & \Rightarrow Z > 34.26 \end{aligned}$$

(the relativistic effects change it slightly.) For such large $Z \geq 35$, we have $F \geq 35 (c/16)^2$, and the corresponding intensities are on the order of $9.0 \cdot 10^{19} (W/cm^2)$, meaning that a laser pulse with very high intensity is required. The second condition of $F < F_a \approx Z^3/16$ for $Z \geq 35$ corresponds to $F_a = 9.4 \cdot 10^{19} (W/cm^2)$ (with relativistic effect $F_a = 9.7 \cdot 10^{19} (W/cm^2)$). However, the thick barrier limit does not need to be taken into account, as this is a multiphoton process (vertical channel). In Fig. 5, we plot Q_{Nad} of Eq. 8 vs. field strength F for various Z . For every Z we let F vary up to $F_a(Z)$, where $F_a(Z) = I_p^2/(4Z)$. However, as given in Eqs. 8, 9 only when $F_c = (c/16)^2 Z < F \leq F_a$ is satisfied superluminality exists, which is conform with the condition $Z \geq 35$ as given in Eq. 9 and clearly seen in fig. 5 (red, orange and green colored curve). For $Z < 35$ we have $F_c > F_a$ and no superluminality can exist (e.g. for $Z = 15, 30$ in fig. 5, the black and blue colored curves). For $F > F_a$ the barrier-suppression-ionization (BSI) region is reached, which will be the subject of future work.

This again shows that the QS of tunnel-ionization requires extreme conditions, now when comparing the time delay τ_{dion} with τ_c^{Nad} , the time it takes for light to travel (horizontally) the same distance x_m that the particle travels horizontally while climbing the potential barrier (vertical channel), compare Fig. 2. Thus, the time-delayed tunnel-ionization of the vertical channel (or the multiphoton process), which is an interaction time-delay (as already mentioned), can be superluminal in the attoclock framework, albeit only under extreme condition, as we have seen in the adiabatic tunneling in sec. II A 0 b.

Concerning the interaction time in this case, the tunnel-ionization (vertical channel) occurs by multiphoton absorption of a number of photons n , and we can assume that $n \approx I_p/\omega$. The time-delay can be written in the form

$\tau_{dion} = \frac{1}{8Z} \frac{n\omega}{F}$, meaning that for the absorption of n photons within the atomic potential we have

$$\tau_{nph} = n \frac{\omega}{8ZF} = n \frac{\pi}{4Z} \frac{1}{FT} = n \frac{1}{\alpha} \frac{\pi}{4Z} \frac{1}{\lambda F}, \quad (10)$$

which can also be written in the form $\tau_{dion} = n \tau_{1ph}$, where τ_{1ph} is the time for the absorption of one photon, where α is the fine structure constant (α is the strength of the light-matter interaction), T the period and λ the wave length of the laser pulse. The relation 10 shows that the time-delay τ_{dion} decreases with increasing strength of the potential, Z , and the period of the laser pulse T . The later property is in contrast to the finding of Esposito [34] and Nitz [18] that the time-delay (phase time) for opaque barrier correlate with reciprocal of the photonic frequency ($\tau \sim 1/\nu = T$) in photonic tunneling. Furthermore, τ_{dion} depends linearly on the barrier width (i.e. on $\frac{I_p}{F} = d_C \approx d_B$ for thick-barrier, compare Eq. 2), which is why Winful's argument mentioned above at the beginning of this section (based on the lack of dependence on the barrier width [22]) is not applicable.

C. The intermediate regime

This is an interesting regime because in this case the two tunnel-ionization channels co-exit [29], adiabatic (horizontal channel) and nonadiabatic (vertical channel), as depicted in Fig. 2 dotted (magenta, purple) curves. Interesting because, as we found in sec. II A, QS is possible in the adiabatic case, but the probability of transmitted particles can be very low. While, as we found in sec. II B, QS is hardly possible in nonadiabatic tunnel-ionization, where the probability of transmitted particles can be assumed to be high (multiphoton absorption), compare Fig. 2 dashed (light blue) curve. Therefore, the intermediate tunnel-ionization can vary with different contributions between the two channels, opening the possibility of QS with different probabilities of the transmitted particles. Nevertheless, we can reasonably describe this regime based on our model, which accurately describes the two regimes mentioned above and our understanding of the last paragraphs II A, II B. It is clear from our discussion that the first term in the model 3 (τ_{dion}) always exist, compare sec. I 0 c, II A and II B. The second term τ_{dB} , the barrier time-delay, which exists in the adiabatic case (Eq. 3), is reduced in the intermediate regime so that it disappears by reaching the vertical channel of the nonadiabatic case, compare Fig. 2.

1. Establishing a model for the intermediate regime

Before we discuss the QS in the intermediate regime in the next subsection, we first introduce the model for studying QS in the intermediate regime in this subsection.

In the intermediate regime, tunnel-ionization can be divided into two parts: partially climbing the barrier to a virtual state corresponds to a contribution from the vertical channel, and crossing the remaining barrier corresponds to

a contribution of the horizontal channel, reaching the tunnel exit point (x_{imed}), as shown in Fig. 2, where three such events are shown (dotted purple or magenta curves). The situation can be described by a dimensionless switching parameter $0 \leq \zeta \leq 1$ and with Eq. 3 one obtains,

$$\tau_{imed} = \tau_{dion} + \zeta \tau_{dB} = \frac{I_p}{8Z_{eff}F} + \zeta \frac{\delta_z}{8Z_{eff}F}, \quad (11)$$

$$d_{imed} = x_m + \zeta(d_B - x_m) = (1 - \zeta)x_m + \zeta d_B, \quad (12)$$

where $Z_{eff} = Z$, d_B is the barrier width, τ_{dB} is the barrier time-delay of Eq. 4, and $\zeta = 0, 1$ correspond to the nonadiabatic and adiabatic case, respectively. The barrier width in this case, denoted d_{imed} with the exit point x_{imed} (compare Fig. 2), is approximated using the same parameter ζ , which is justified because the tunnel-ionization time-delay (in particular τ_{dB} , Eq. 3 and 4) depends linearly on the barrier width. This is justified as long as $F \leq F_a$ holds, where $d_B \geq x_m$; furthermore, our focus is on the limit $F \ll F_a$, compare fig 6. The limits $\zeta = 0$ and $\zeta = 1$ correspond to the two cases given in II B 0 b, II A, since $\lim_{\zeta \rightarrow 0,1} \tau_{imed} = \tau_{dion}, \tau_{Ad}$, and $\lim_{\zeta \rightarrow 0,1} d_{imed} = x_m, d_B$ respectively.

To verify the reliability of our model in Eq. 12, we plot in Fig. 6 (a) the exit point x_{exit} of different approaches for hydrogen atom versus field strength F . We take the limit of thick barrier, where $d_B = d_C$ (which is commonly used in the literature) and $d_{imed} \approx x_{e,imed}$. As a test we set $\zeta = 0.5$ and plot $x_{e,imed}(\zeta = 0.5)$ (denoted PW with $\zeta = 0.5$, dark green colored in Fig. 6 (a)) together with a model of exit point of NITDSE recently published in [35] by Ivanov et. al. (red colored with error bars, see ref. [35]), and a model of Li et al [36] (black colored in Fig. 6 (a)). Also shown the exit points of the adiabatic $x_{e,+}$ (light green) and nonadiabatic x_m (orange) cases of our model (see sec. I). The agreement of our model for the hydrogen atom with $\zeta = 0.5$ as a test with the results given in the literature, in particular the NITDSE from ref. [35], shows that our model is reliable and can serve as a generalized model, although ζ is a parameter that needs to be precisely determined. Further information, possibly from experiments, is required for this.

2. QS in the intermediate regime

We will investigate the QS for the intermediate tunnel-ionization with the help of Eqs. 11, 12 which, as we will see, shows interesting features. Its behavior at the boundaries $\zeta = 0, 1$ coincides with the two cases given of sec. II B 0 b, II A 0 b, respectively. As before, we take the thick-barrier ($F \ll F_a$), where $\delta_z \approx I_p$, $d_B \approx d_C = I_p/F$, and first compare τ_{imed} with $\tau_c^{Ad} = d_C/c = I_p/cF$, later with $\tau_c^{imed} = d_{imed}/c$.

a. *With τ_c^{Ad} :* In this case and from Eq. 11, we obtain the following condition for superluminality,

$$Q_{imed}^a = \frac{\tau_{imed}}{\tau_c^{Ad}} = \frac{c(1 + \zeta)}{8Z} \leq 1, \Rightarrow Z \geq \frac{c(1 + \zeta)}{8} \quad (13)$$

which leads to $Z \geq Z_\zeta = (c/8)(1 + \zeta)$, where $Z_\zeta \approx 17.13 - 34.26$ for $0 \leq \zeta \leq 1$ and field strength $F < F_a$ (or $F \ll F_a$ thick-barrier). The tunnel-ionization is for $Z \leq 17$ subluminal, see sec. II B 0 a.

An increase in ζ increases the Z value (equation 13) and the adiabatic contribution, with the occurrence of superluminal speed depending on the ζ value. We illustrate this in

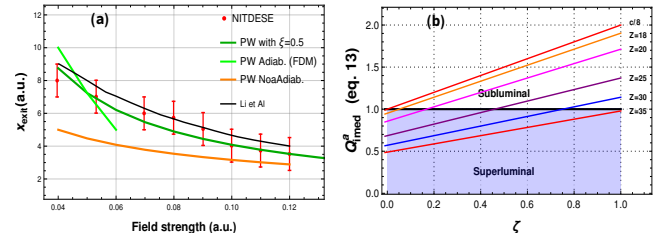


FIG. 6. (Color online) (a): The plot shows the exit point (in au) of different approaches for hydrogen atom versus field strength F (in au), see Figs. 1, 2, sec. I and Eq. 12. (b): Q_{imed}^a (Eq. 13) vs. ζ for selected Z -values showing transition from subluminal to superluminal (see text).

Fig. 6 (b), where we plot Q_{imed}^a vs. ζ for selected Z values, which shows the linear dependence on ζ (Eq. 13). As seen in Fig. 6 (b), for a given Z (e.g. Z_i) or a segment (Z_i, ζ) superluminal tunnel-ionization (colored area) exists as long as ζ is below a value ζ_i , which is determined by the intersection with the black line $Q_{imed}^a = 1$, which is given by $\zeta_i = -1 + 8Z_i/c$. Or for a chosen Z_i , the tunnel-ionization is subluminal when $\zeta > \zeta_i$. Conversely, QS (colored area) exists for a given value ζ_i (at an intersection with the black line) for all Z values larger than Z_i that corresponds to ζ_i . This can be seen for a chosen ζ_i (on the black line) through a vertical line at ζ_i on the ζ -axis in Fig. 6 (b). At $\zeta = 1$ (or $\zeta_i = \zeta_{35}$) the QS satisfies the condition of Eq. 7 (i.e. the adiabatic tunnel-ionization is superluminal for all $Z \geq 35$) as clearly seen in Fig. 6 (b) (colored area) and already discussed in sec. II A 0 b. While on the opposite side, i.e. $\zeta = 0$, QS is only possible for $Z \geq 18 \approx c/8$, which corresponds to the nonadiabatic tunnel ionization case described in II B 0 a.

However, the superluminality discussed here is based on our probably erroneous definition through the use of τ_c^{Ad} , which is justified only for the adiabatic case with $\zeta = 1$. See also discussion in in sec. II B 0 a.

b. *With τ_c^{imed} :* The comparison in the previous paragraph II C 2 a is questionable, because the barrier width d_B (or d_C) was used, whereas the corresponding horizontal distance to the exit point x_{imed} (see Fig. 2) is given by d_{imed} . And $\tau_c^{imed} = d_{imed}/c$ is then the time that the light needs to travel (horizontally) the distance d_{imed} (Eq. 12).

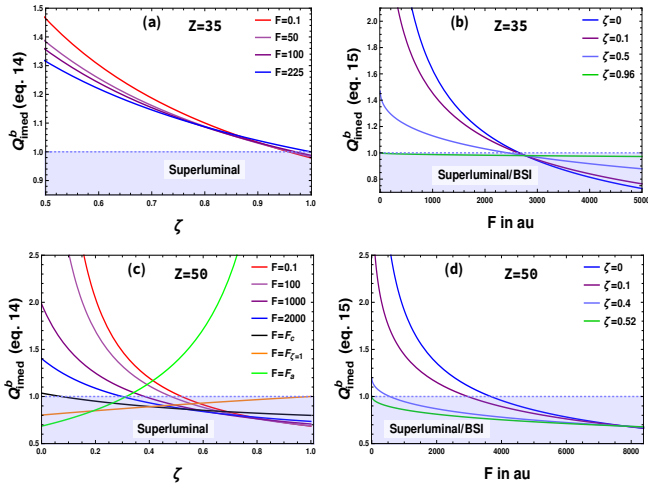


FIG. 7. (Color online) (a),(c): Q_{imed}^b of Eq. 14 vs. ζ for $Z = 35, 50$ for different field strengths, showing transition from subluminal to superluminal at the corresponding ζ_{QS} . In (c): $F_c = 3667.75 au$ (Eq. 9), $F_{\zeta=1} = 6104.5 au$ and the atomic field strength $F_a = 8380.3 au$ (see text). (b),(d) Q_{imed}^b of Eq. 15 vs. field strength for $Z = 35, 50$ for different ζ values.

Therefore, with Eqs. 11, 12 we obtain:

$$\begin{aligned}
 Q_{imed}^b(Z, \zeta, F) &= \frac{\tau_{imed}}{\tau_c} \\
 &= \frac{c(I_p + \zeta \delta_z)}{(8ZF)(1 - \zeta)x_m + 8\zeta Z \delta_z} \quad (14) \\
 &= \frac{c(1 + \zeta)}{(8ZF/I_p)(1 - \zeta)x_m + 8\zeta Z} \quad (15) \\
 &\approx \frac{c(1 + \zeta)}{16(1 - \zeta)/x_m + 8\zeta Z} \quad (16)
 \end{aligned}$$

with $\zeta \in [0, 1]$, where in the 3rd line the thick barrier limit $\delta_z \approx I_p$ (thick-barrier limit) and in the 4th line $I_p = Z^2/2$ is used. From Eqs. 14-16 it can be verified that the limits $\zeta \rightarrow 1, 0$ give the two cases discussed above in sec II A 0 b and II B 0 b, with the condition $Q_{imed}^b \leq 1 \Rightarrow Z \geq c/4 \approx 34.26$ for the two limits. In other words, the condition of $Z \geq 35$ for the QS to happen, is the same regardless of the contributions of vertical and horizontal channels. We note that it can be shown that (where $F > 0$) for $0 < Z \leq c/8$, $\zeta < 0$ and for $c/8 < \zeta < c/4$, $\zeta < 0$ or $\zeta > 1$, i.e. values that lie outside the range are obtained.

In Fig. 7 (a), (c) Q_{imed}^b of the equation 14 is plotted against ζ for $Z = 35, 50$ and various field strengths and in Fig. 7 (b),(d) Q_{imed}^b of the equation 15 against the field strength for $Z = 35, 50$ and various ζ values, respectively. We first discuss Fig. 7 (a), (c) and then return to Fig. 7 (b),(d) later.

In the following, ζ_{QS} denotes the value of ζ at the intersection with the dotted line at $Q_{imed}^b = 1$ in Fig. 7(a)-(d), which can be determined by solving of the equation $Q_{imed}^b(Z, \zeta, F) = 1$ of Eq. 14 or 15 with the corresponding Z and F values.

Considering Fig. 7 (a),(c) we see that a main feature is that the adiabatic and nonadiabatic contributions (i.e. ζ value) for which the QS occurs, changes with the field strength. Furthermore, it is evident that for $F \sim 0$ quantum superluminality depends also on Z values. At the lower value of $Z = 35$ (Fig. 7(a)), QS is only possible for $\zeta_{QS} \sim 1$, which corresponds to the adiabatic or horizontal channel. For $Z = 35$ this channel is hardly possible at such field strengths (since it is the multiphoton regime because the Keldysh parameter is too large $\gamma_K = \omega \sqrt{2I_p}/F \gg 1$, where ω is the laser frequency and it is of order $1 - 3 a.u.$). This means that at field strengths $F \sim 0$, the probability amplitude for such a process is expected to be very small. While ζ_{QS} changes slowly with increasing F values, the probability amplitude is expected to increase as a result.

For larger Z , as we see in Fig. 7(c) for $Z = 50$, the situation changes and QS occurs at smaller ζ_{QS} values and changes gradually with F , where for small field strength we have $\zeta_{QS}(F \sim 0) \approx 0.52$, the solution of $Q_{imed}^b(Z = 50, \zeta, F \sim 0) = 1$. At higher field strengths as $\zeta_{QS}(F)$ decreases, the adiabatic contribution decrease, while the multiphoton contribution increases and QS occurs at the corresponding $\zeta_{QS}(F)$ value. Once the field strength reaches $F_c = (c/16)^2 Z$ (compare Eq. 9), QS becomes already possible at $\zeta(F_c) \sim 0$ (and for $\zeta \geq 0$, black curve in Fig. 4(c)), where the nonadiabatic tunnel-ionization or the vertical channel is superluminal as we have seen in section II B 0 b, and an additional contribution from the horizontal channel is then no longer so important. This trend continues as F increases until $F_i = F_{\zeta=1}$, which is the solution of $Q_{imed}^b(Z_i, \zeta = 1, F) = 1$ with the corresponding $Z = Z_i$ value ($Z_i = 50$ in our case, orange colored line in Fig. 7 (c)).

For larger field strengths $F_{\zeta=1} < F < F_a$ the trend turns now in the opposite direction and the vertical channel (nonadiabatic contribution) is gaining in importance and QS occurs at $\zeta_{QS} < 1$ values until $F = F_a$ with the smallest value $\zeta_{QS}(F_a)$ (green curve in Fig. 7 (c), where $\zeta_{QS}(F_a)$ is the solution of $Q_{imed}^b(Z_i, \zeta, F_a) = 1$ (in our case of $Z = 50$, $\zeta_{QS}(F_a) \approx 0.31$), where the QS is then possible for $\zeta \leq \zeta_{QS}(F_a)$ at $F = F_a$ although $\delta_z = 0$ (compare Eq. 14). However, for $F > F_a$ (BSI) the QS (of Q_{imed}^b) becomes imaginary but for $\zeta = 0$, because δ_z becomes imaginary.

The comparison between the two cases in figure 7 (a), (c) shows that as Z increases, the ζ values at which superluminal speed occurs decrease. This can be easily derived from Eq. 14; for example, for every F , $\zeta(Z_2, F) < \zeta(Z_1, F)$ is obtained if $Z_2 > Z_1$. The higher Z is, the smaller the ζ value at which the intersection with $Q_{imed}^b = 1$ occurs (as can be seen from Eq. 14-16 by setting $Q_{imed}^b = 1$). Otherwise, as Z increases, the behavior for all $Z > 35$ approaches that of the value $Z = 50$ in Fig. 7 (c) and remains similar for all large $Z > 35$.

It worth noting that the above discussed behavior of tunnel-ionization actually differs from known studies on tunneling (usually on system with small Z or Z_{eff}), where adiabatic and nonadiabatic channel are even studied experimentally separately, see e.g. [12] and the references

therein, referred to as adiabatic and nonadiabatic field calibration. Therefore, we think that the approximations in Eqs. 11,12 suggest to investigate tunnel-ionization mechanism, where the two channels contribute to the tunneling, compare Fig. 6 (a). In fact, this has already been discussed in earlier works on tunneling mechanism, e.g. by Ivanov et al. [29], who proposed the coexistence of horizontal and vertical channels, as outlined in Fig. 2 (intermediate curves).

We now turn to Fig. 7 (b), (d), where we plotted Eq. 15 (where the approximation $\delta_z = I_p$ and $d_B \approx d_C$ are used) against the field strength F for various ζ values. As can be seen from the figures, similar features are observed as in Fig. 7 (a), (c). For smaller Z , i.e. $Z = 35$ in Fig. 7 (b), for small field strengths superluminal tunnel-ionization only occurs for $\zeta \sim 0.96$ value, i.e. near the adiabatic limit (green curve in Fig. 7 (b)). Otherwise it occurs at exclusively large field strengths for all ζ value smaller that $\zeta_{QS} \approx 0.96$, which is found by solving $Q_{imed}^b = 1$ of Eq. 15 and taking the limit at small F , which changes only slightly with increasing field strength F . With further increasing field strength, barrier suppression ionization (BSI) is reached, in which QS also occurs. It should be noted, however, that in Eq. 15 $d_C = I_p/F$ is used instead of $d_B = \delta_z/F$ (see Eq. 12).

For larger Z , e.g. $Z = 50$ in Fig. 7 (d), we observe a similar behavior but ζ_{QS} becomes smaller with increasing Z value and changes significantly with increasing field strength F . At small or realistic field strengths of $F \sim 100 - 500$, the value is approximately $\zeta_{QS} \sim 0.52$ (green curve in Fig. 7 (d)), where the adiabatic and nonadiabatic contributions are sufficiently balanced, compare Fig. 6 (a). For small ζ_{QS} values, the probability of superluminal tunnel-ionization can be high, as this corresponds to the multiphoton regime (blue and purple colored curves in Fig. 7(d)). However, the field strengths needs to be too high for this to occur.

Our final result is shown in Fig. 8. There, the tunnel-ionization time-delay τ_{imed} and the corresponding τ_c^{imed} are plotted as a function of F for small and experimentally reliable field strengths for selected Z values. For clarity in Fig. 8, a slightly larger ζ -value than ζ_{QS} for the corresponding Z is used, which as already mentioned is determined from Eq. 14 by solving the equation $Q_{imed}^b = 1$ and taking the limit for small F (compare Fig. 7(a),(c)). As can be seen in Fig. 8, the curves for τ_c^{imed} (green dotted curves) are somewhat higher or above the respective τ_{imed} (i.e. $\tau_{imed} < \tau_c^{imed}$), which becomes more apparent the larger Z is. For the smaller Z values, i.e. $Z = 35$, $\zeta_{QS} \approx 0.96$ the tunnel-ionization happens almost adiabatic (horizontal channel). The adiabatic contribution is only slightly below its maximum at $\zeta = 1$, however, it is not expected that the probability of tunnel ionization will be significantly increased compared to adiabatic tunnel ionization (corresponding to $\zeta = 1$).

As already mentioned (compare Fig. 7 (a),(c)), a decrease in ζ , although it implies an increase in Z , means a decrease in the adiabatic contribution, where one would expect an increase in the tunnel-ionization probability (despite that the barrier becomes thicker and higher) as multiphoton absorption (vertical channel) becomes important. For

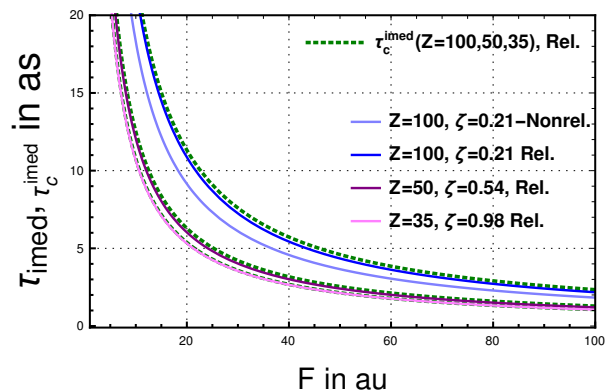


FIG. 8. (Color online) Time-delay τ_{imed} (Eq. 11) for $Z = 35, 50, 100$ values and the corresponding $\tau_c^{imed} = d_{imed}/c$ (green dashed for all Z), see Eq. 12 and sec. II C 2 b, vs. field strength F , showing QS for $Z \geq 35$ for different (Z, ζ) -values.

$Z = 50$, we find $\zeta_{QS} \sim 0.52$ for the occurrence of QS at small field strength, so that the two adiabatic/nonadiabatic contributions are in a balanced ratio. This represents a case that appears experimentally feasible, and its experimental investigation and confirmation would be an important step and an insightful finding for tunnel theory in general. With a further increase in the Z value, e.g. $Z = 100$ shown in Fig. 8, QS becomes even more pronounced, such that the non-adiabatic contribution predominates (since $\zeta_{QS} \sim 0.2$ is relatively small). However, for such a large Z , the barrier becomes too thick at small field strengths, and the probability amplitude for such a process would likely be small.

D. Summary

In summary, our approach is consistent and provides evidence for, or clarifies, the QS of tunnel-ionization. Our result represents an important step towards understanding this fundamental physical property of tunnel-ionization; experimental verification using the attoclock scheme is possible, albeit under somewhat strict conditions. We summarize our result for H-like atomic ions as follows:

1. In the adiabatic case, sec II A (see Fig. 2 red dashed-dotted curve), the QS is a fundamental property of adiabatic tunnel-ionization. We found that the barrier time-delay (compare Eqs. 4, 6 and Fig. 3) exhibits QS if $Z \geq 18$ at field strengths $F \leq F_a$. However, the probability for such process is most likely to be low [14, 19, 33].
2. In the nonadiabatic case, sec. II B (see Fig. 2 (dashed light blue curve), we found that the tunnel-ionization or interaction time-delay is superluminal under the condition $Z \geq 35$, $F \geq F_c = (c/16)^2 Z$ when τ_c^{Nad} is correctly defined by using the correct barrier width, which corresponds to $d_m \approx x_m$, as shown in II B 0 b.
3. The intermediate case, sec. II C (see Fig. 2 magenta and purple dotted curves), is important from both

fundamental and experimental (or application) point of view. It actually represents the general case, which includes also the two limiting cases, the adiabatic and nonadiabatic case. We found in sec. II C 2 b that under the relatively stringent condition $Z \geq 35$, $0 \leq \zeta \leq 1$ (compare Eq. 14, 15), the QS occurs with a varying adiabatic/nonadiabatic contribution dependent on ζ . However, ζ becomes small for larger Z (e.g., $Z = 50$ in Fig. 7(c),(d)). Since this implies a decrease in the ratio of adiabatic to non-adiabatic (multiphoton) contribution, an increase in the tunnel-ionization probability is to be expected.

4. Our final result is shown in Fig. 8. It clearly demonstrate the possibility of QS in tunnel-ionization. Although the conditions are somewhat strict, the result can be experimentally investigated using the attoclock framework, especially that the field strengths for such a process are available.

The probability or the electron momentum distribution of tunnel-ionization requires a separate investigation in all of these cases. Furthermore, an important result is found in

sec. II A, where the QS condition for the barrier time τ_{dB} of Eq. 4 is less severe ($Z \geq 18$), as shown in Eq. 6 and Fig. 3. Although τ_{dB} cannot be measured directly, it can be extracted from the two calibrations (adiabatic and nonadiabatic) of the same experimental result, in a similar way to the experimental result of the He atom [3, 4] as shown in our previous work, compare fig 3 in [12]. The barrier time-delay τ_{dB} corresponds to the well known dwell time in the framework of UTTP [12–14], and to the LC time-delay and the interaction time (in the weak measurement and thick-barrier limit) [32, 37–39]. The thick-barrier limit $\delta \approx I_p$ have a negligible effect in our approach because $I_p \sqrt{1 - 4FZ/I_p^2} \approx I_p$ for large Z and small field strength. Experimentally, verifying these results using the attoclock scheme is straightforward, as the required field strengths are available. Carrying out the experiment on H-like atoms with large Z could be difficult, but we think it does not represent a major obstacle.

Acknowledgments I would like to thank Prof. Martin Garcia from the Theoretical Physics of the Institute of Physics at the University of Kassel for his kind support.

-
- [1] O. Kullie, *Phys. Rev. A* **92**, 052118 (2015), arXiv:1505.03400v2.
 - [2] O. Kullie and I. A. Ivanov, *Annals of Physics* **464**, 169648 (2024).
 - [3] A. S. Landsman, M. Weger, J. Maurer, R. Boge, A. Ludwig, S. Heuser, C. Cirelli, L. Gallmann, and U. Keller, *Optica* **1**, 343 (2014).
 - [4] C. Hofmann, A. S. Landsman, and U. Keller, *J. Mod. Opt.* **66**, 1052 (2019).
 - [5] S. Augst, D. Strickland, D. D. Meyerhofer, S. L. Chin, and J. H. Eberly, *Phys. Rev. Lett.* **63**, 2212 (1989).
 - [6] S. Augst, D. D. Meyerhofer, D. Strickland, and S. L. Chin, *J. Opt. Soc. Am. B* **8**, 858 (1991).
 - [7] N. B. Delone and V. P. Kraїnov, *Phys.-Usp.* **41**, 469 (1998).
 - [8] I. Y. Kiyan and V. P. Kraїnov, *Soviet Phys. JETP* **73**, 429 (1991).
 - [9] O. Kullie, *Journal of Physics B: Atomic, Molecular and Optical Physics* **49**, 095601 (2016).
 - [10] O. Kullie, *Ann. of Phys.* **389**, 333 (2018), arXiv:1701.05012.
 - [11] O. Kullie, *Quant. Rep.* **2**, 233 (2020).
 - [12] O. Kullie, *Journal of Physics Communications* **9**, 015003 (2025).
 - [13] H. G. Winful, *Phys. Rev. Lett.* **91**, 260401 (2003).
 - [14] J. T. Lunardi and L. A. Manzoni, *J. Phys.: Conference Series* **1391**, 012112 (2019).
 - [15] T. E. Hartman, *J. Appl. Phys.* **33**, 3427 (1962).
 - [16] P. Balcou and L. Dutriaux, *Phys. Rev. Lett.* **78**, 851 (1997).
 - [17] W. Heitmann and G. Nimtz, *Physics Letters A* **196**, 154 (1994).
 - [18] G. Nimtz and A. Stahlhofen, *Annalen der Physik* **520**, 374 (2008), arXiv:0901.3968.
 - [19] R. S. Dumont and T. Rivlin, *Phys. Rev. A* **107**, 052212 (2023).
 - [20] R. Y. Chiao and A. M. Steinberg, in *Progress in Optics*, Vol. 37, edited by E. Wolf (Elsevier Publishing, 1997) pp. 345–405.
 - [21] R. Y. Chiao, *AIP Conference Proceedings* **461**, 3 (1999), arXiv:9811019.
 - [22] H. G. Winful, *Nature* **424**, 638 (2003).
 - [23] H. G. Winful, *Phys. Rev. Lett.* **90**, 023901 (2003).
 - [24] M. Büttiker and S. Washburn, *Nature* **422**, 271 (2003).
 - [25] A. M. Steinberg, P. G. Kwiat, and R. Y. Chiao, *Phys. Rev. Lett.* **71**, 708 (1993).
 - [26] L. A. MacColl, *Phys. Rev.* **40**, 621 (1932).
 - [27] L. Nanni, *Pramana* **97**, 37 (2023).
 - [28] J. T. Lunardi and L. A. Manzoni, *Advances in High Energy Physics* **2018**, "ID1372359" (2018).
 - [29] M. Y. Ivanov, M. Spanner, and O. Smirnova, *J. Mod. Opt.* **52**, 165 (2005).
 - [30] A. S. Landsman and U. Keller, *Phys. Rep.* **547**, 1 (2015).
 - [31] E. Clementi and D. L. Raimondi, *J. Chem. Phys.* **38**, 2686 (1963).
 - [32] D. C. Spierings and A. M. Steinberg, *Phys. Rev. Lett.* **127**, 133001 (2021).
 - [33] H. G. Winful, *Physics Reports* **436**, 1 (2006).
 - [34] S. Esposito, *Phys. Rev. E* **64**, 026609 (2001).
 - [35] I. A. Ivanov, A. S. Kheifets, and A. S. Landsman, *J. Opt. Soc. Am. B* **42**, 1878 (2025).
 - [36] M. Li, J.-W. Geng, M. Han, M.-M. Liu, L.-Y. Peng, Q. Gong, and Y. Liu, *Phys. Rev. A* **93**, 013402 (2016).
 - [37] M. Büttiker, *Phys. Rev. B* **27**, 6178 (1983).
 - [38] A. M. Steinberg, *Phys. Rev. Lett.* **74**, 2405 (1995).
 - [39] R. Ramos, D. Spierings, I. Racicot, and A. M. Steinberg, *Nature* **583**, 529 (2020).
 - [40] I. A. Ivanov and A. S. Keifets, *Phys. Rev. A* **89**, 021402 (2014).

- [41] I. A. Ivanov, J. Dubau, and K. T. Kim, *Phys. Rev. A* **94**, 033405 (2016).
 [42] M. Nurhuda and F. H. M. Faisal, *Phys. Rev. A* **60**, 3125 (1999).

Appendix A

1. Numerical Integration of the Time-Dependent Schrödinger Equation

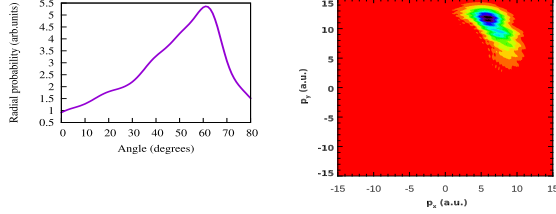


FIG. 9. (Color online) Photo-electron momentum distribution in the polarization plane, and radially integrated distribution defined by eq A5. Field and target parameters: $Z = 18$, $F_0 = 50 au$, $\omega = 3 au$.

We follow closely the numerical procedure we used to solve the TDSE in [40, 41]. We solve the TDSE for a single-electron atom with an effective central potential: $V(r) = -\frac{Z_{eff}}{r}$ in the presence of a laser pulse:

$$i\frac{\partial\Psi(\mathbf{r})}{\partial t} = \left(\hat{H}_{\text{atom}} + \hat{H}_{\text{int}}(t)\right)\Psi(\mathbf{r}). \quad (\text{A1})$$

We use velocity form for the operator $\hat{H}_{\text{int}}(t)$ describing interaction of the atom with the laser field:

$$\hat{H}_{\text{int}}(t) = \mathbf{A}(t) \cdot \hat{\mathbf{p}}, \quad (\text{A2})$$

where $\mathbf{A}(t) = -\int_0^t \mathbf{E}(\tau) d\tau$ is the vector potential of the laser pulse, which for the geometry we employ (with quantization axis and pulse propagation direction along the z -axis), is defined as follows:

$$\begin{aligned} A_x(t) &= -\frac{f(t)F_0}{\omega\sqrt{1+\epsilon^2}}\cos\omega t, \\ A_y(t) &= \frac{\epsilon f(t)F_0}{\omega\sqrt{1+\epsilon^2}}\sin\omega t, \end{aligned} \quad (\text{A3})$$

where $\epsilon = 1$ is ellipticity of the pulse, F_0 its field strength (not to be confused with the *peak field strength* F which we use in the formulas in the main text). The function $f(t)$ in eq A3 is the pulse envelope which we chose as: $f(t) =$

$\sin^{16}(\pi t/T_1)$, where $T_1 = 2T$, with $T = 2\pi/\omega$ - an optical cycle corresponding to the fundamental frequency ω , is a total duration of the pulse. The initial state of the system is the ground $1s$ state of an atom with effective potential $V(r) = -\frac{Z_{eff}}{r}$. Solution of the TDSE is represented as a series in spherical harmonics:

$$\Psi(\mathbf{r}, t) = \sum_{l,m} f_l(r, t) Y_l^m(\theta, \phi), \quad (\text{A4})$$

where spherical harmonics with orders up to $L_{\text{max}} = 100$ were used for the field strength F_0 we employed in the calculations. The radial variable is treated by discretizing the TDSE on a grid with the step-size $\delta r = 0.1$ a.u. in a box of the size $R_{\text{max}} = 400$ a.u. Necessary checks were performed to ensure that for these values of the parameters L_{max} and R_{max} convergence of the calculations has been achieved. The wave-function $\Psi(\mathbf{r}, t)$ was propagated in time using the matrix iteration method [42].

Ionization amplitude into a photo-electron state with asymptotic momentum \mathbf{p} is computed by projecting the solution of the TDSE $\Psi(\mathbf{r}, T_1)$ at the end of the laser pulse on the scattering states $\phi_{\mathbf{p}}$ with ingoing boundary conditions.

We are interested in photo-electron momenta distribution $P(p_x, p_y, 0)$ in the polarization (p_x, p_y) -plane. In Fig. 9 a typical distribution is shown using the procedure we described above. An observable we are after is the offset angle, which for the pulse defined by eq A3 is the angle between the negative y - direction and the ray pointing at the maximum of the photo-electron momentum distribution. To extract the offset angle, we follow the strategy we employed in [40]. We compute the radially integrated distribution $P(\phi)$ defined as:

$$P(\phi) = \int_0^\infty P(p_x, p_y, 0) p dp, \quad (\text{A5})$$

where $p = \sqrt{p_x^2 + p_y^2}$, factor p under the integral sign in eq A5 appears because of the area element in the (p_x, p_y) -plane, and angle ϕ is measured from the positive x - direction.

2. Result

In Fig.2, the numerical result of the photo-electron momenta distribution and the the radially integrated distribution $P(\phi)$ for $Z = 18$, $F = 50 a.u.$ and $\omega = 3 a.u.$ are shown. From the the radially integrated distribution we obtain a time-delay of $\sim 4 as$.

Unfortunately, this value is slightly larger than the corresponding time-delay resulting from our model $\tau_{dion} \sim 1 as$. We do not know at the moment the reason behind this discrepancy. Further calulatiois are in prgress.